On the Crystal Structure of Nylon 55

Eloísa Navarro, C. Alemán, J. A. Subirana, and Jordi Puiggalí*

Departament d'Enginyeria Química, ETS d'Enginyers Industrials, Universitat Politècnica de Catalunya, Diagonal 647, Barcelona 08028, Spain

Received January 2, 1996; Revised Manuscript Received April 18, 1996[®]

ABSTRACT: The structure and morphology of nylon 55 has been investigated using transmission electron microscopy, selected area electron diffraction, and X-ray diffraction. Different morphologies, varying from rhombus to lath-shaped lamellar crystals, were obtained from formic acid−butanol solutions. The unit cell is monoclinic with dimensions $a = 8.30$ Å, $b = 4.79$ Å, c = 13.8 Å, and $\alpha = \beta = \gamma = 90°$. The space group is probably $C121$, which is noncentrosymmetric. The conformation of nylon 55 has been analyzed with the linked-atom least-squares (LALS) methodology applied to X-ray and electron diffraction data and with quantum mechanical calculations. A molecular conformation where the two amide groups of the repeating unit are ca. 120° rotated seems to be stabilized with respect to a conventional γ-form. The molecules are packed in a network of hydrogen bonds with two spatial orientations, similarly to the proposed structures for nylon 65 and nylons n,3. This packing differs from the conventional structure for the α and γ forms of nylons where a single hydrogen bond direction is found.

Introduction

Although nylons have been known for well over 60 years, there still remains considerable confusion in the literature concerning the nature and stability of their crystalline structures (i.e., more than 10 and seven different unit cells have been given[1] for nylons 6 and 66, respectively). However, the structures reported at low temperature are characterized by a single hydrogen bond direction and can be classified into two groups: (a) The α- and β-forms constituted by hydrogen-bonded sheets with fully extended chains and (b) the γ-form, also constituted by hydrogen-bonded sheets, but with a pleated-sheet structure, corresponding to a pseudohexagonal unit cell or one very close to it. Transformations between both kinds of structures can be engineered in some cases by solvent or swelling agents,[2] rates of fiber spinning,[3] and temperature.[4] Structural variations can be envisaged as a consequence of different possible balances between the van der Waals attractions, hydrogen bonds, dipole−dipole forces, and torsion about covalent bonds. Thus in nylons derived from ω-amino acids and with more than six methylene groups between the amide groups, the dominance of the van der Waals forces over the hydrogen bonds is such that the extended conformation seldom exists.

The pseudohexagonal phase is particularly confusing since it may or may not yield an α-form upon annealing under pressure (i.e., nylons 6[5] and 12[6]), depending on the way in which it was previously obtained. In such cases the structure that is transformable into the α-form is called γ' to distinguish it from the nonreversible γ-form. On the other hand Atkins *et al.*[7] obtained a pseudohexagonal form of nylon 8 by rapid quenching from the crystallization temperature into a nonsolvent, which was interpreted as a trigonal arrangement of hydrogen bonds produced when the amide groups flip $\pm60°$ out of the planar chain conformation. A pseudohexagonal modification may be also attained when nylons are heated above the "Brill transition temperature". Different explanations for the high-temperature form appear in the literature,[8−12] varying from a three-dimensional network of hydrogen bonds to a single hydrogen bond direction.

Recently, we have studied a group of polyamides in which an isolated methylene group is placed between two amide groups. In all cases a pseudohexagonal packing is characteristic. However, the experimental data point to structures with either three,[13−17] two,[18,19] or one[20−22] hydrogen bond direction which are different from the conventional γ-form. The conformational preferences of glycine ($-NHCH_2CO-$), methylenediamine ($-NHCH_2NH-$), and malonyl ($-COCH_2CO-$) residues play a decisive role and strongly influence the final structure. Crystallographic and quantum mechanical studies on model compounds[23−29] support these new structures and also reveal that some dicarbonylic units such as malonyl, succinyl, and glutaryl residues tend to be in a folded conformation where the two C−O directions are rotated. In this sense we have recently reported a new structure with two hydrogen bond directions for nylon 65,[30] which differs from the expected γ-form for even−odd nylons (Kinoshita[31]).

In the present work we study nylon 55 as a representative of odd−odd nylons derived from glutaric acid. Up to the present time no diffraction data have been available for nylon 55 except from Magill,[32] who reported a hexagonal electron diffraction pattern from spherulitic aggregates, and Dreyfuss,[33] who reported its chain repeat as 13.8 Å and its lamellar long spacing as 59 Å, both values measured by X-ray diffraction data. Additional interest in the crystalline structure of nylon 55 derives from its expected pyroelectric and piezoelectric properties.

Experimental Section

Synthesis and Characterization. Nylon 55 was synthesized by interfacial polycondensation of 1,5-diaminopentane and glutaryl dichloride. Approximately 30 mmol of the dichloride dissolved in 150 mL of toluene was added dropwise to a stirred solution of 30 mmol of 1,5-diaminopentane and 120 mmol of NaOH in 150 mL of water. After addition was complete, stirring was continued for 30 min. The polymer which precipitated was isolated by filtration and washed successively with water, ethanol, and ethyl ether before drying in a vacuum desiccator at 60 °C.

The intrinsic viscosity of the polymer was determined by measurements with a Cannon-Ubbelohde microviscometer in dichloroacetic acid solutions at 25 ± 0.1 °C. The density of the powder sample was measured at 25 °C by the flotation method in mixtures of ethanol and carbon tetrachloride. The chemical constitution of the polymer was ascertained by infrared and NMR spectroscopy and elemental analysis. Infrared absorption spectra were recorded from potassium bromide pellets with a Perkin-Elmer 783 spectrometer in the $4000-500$ cm^{-1} range. NMR spectra were registered from
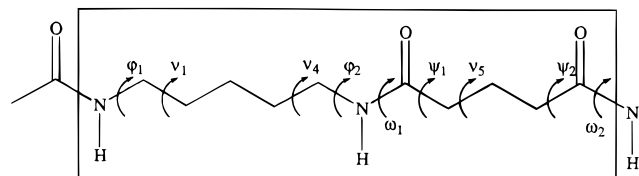
Figure 1. Representation of a nylon 55 repeat unit with a definition of the torsional angles used in Table 2.

polymer solutions in deuterated trifluoroacetic acid using a Bruker AMX-300 spectrometer operating at 300.1 MHz for ^{1}H NMR and at 75.5 MHz for ^{13}C NMR.

Thermal behavior was investigated with a Perkin-Elmer DSC-4 equipped with a TADS data station at a heating rate of 20 °C/min in a nitrogen atmosphere. The instrument was calibrated for temperature (T) and heat of fusion (ΔH) using an indium standard ($T_m = 429.5$, $\Delta H_m = 3.267$ kJ/mol). The expected accuracy is $1-2$ K for T and $\pm 3\%$ for ΔH. A base line was always run and subtracted to avoid the effects of the changing environment.

Structural Methods. Crystallization experiments were carried out isothermally from dilute solutions (0.05−0.1% (w/v)) in formic acid−butanol mixtures. The crystals were recovered from mother solutions by centrifugation and were repeatedly washed with 1-butanol.

For electron microscopy the crystals were deposited on carbon-coated grids, which were then shadowed with Pt−carbon at an angle of 15°. A Philips EM-301 electron microscope operating at either 80 or 100 kV for bright field and electron diffraction modes, respectively, was used throughout this work. Electron diffraction diagrams were recorded by the selected area method on Kodak Tri-X films. The patterns were internally calibrated with gold ($d_{111} = 2.35$ Å).

X-ray diagrams were recorded under vacuum at room temperature, and calcite ($d_B = 3.035$ Å) was used for calibration. A modified Statton camera (W. R. Warhus, Wilmington, DE) with Ni-filtered Cu Kα radiation of wavelength 1.542 Å was used for these experiments. Patterns were recorded from either polymer powders, fibers, or mats of single crystals which were prepared by slow filtration of a crystal suspension on a glass filter.

The diffraction intensities were measured with a Joyce Loebl MK III CSD microdensitometer and were corrected for area, Lorentz, and polarization factors.

Molecular Simulation. Approximate models with a sound stereochemistry were built and then refined using the LALS methodology.[34] The description of a generic residue of nylon 55 is given in Figure 1. Standard bond lengths and angles for polyamides were adopted to build the repeating unit and were fixed throughout the whole modeling process. The torsional angles ν_i and ω_i were kept in the trans conformation, as is usual in polyamides. Therefore, only the four torsional angles next to the amide groups (φ_i and ψ_i) and the positional parameters which fix the chain in the unit cell were needed to define the chain conformation and the packing analysis. The models were refined according to the experimental chain repeat length, the packing constraints due to the unit cell dimensions, and the optimum hydrogen bond geometry. Diffraction data were also used to test the quality of the models. Calculated structure factors were corrected by an isotropic temperature factor ($B = 5$ Å²). X-ray and electron diffraction patterns were also simulated with the CERIUS 3.1 version (Molecular Simulations Inc.). The peaks in the X-ray patterns were broadened with a Lorentzian profile in order to take into account the crystal size. Calculations were run on a HP-340 computer and a Silicon Graphics Indigo workstation.

Energy Calculations. Stereochemically satisfactory models were subject to an energy analysis. Thus, the structural features found from LALS refinements were studied using two well-known semiempirical methods: AM1[35] and PM3,[36] which have very different characteristics. The goodness of the AM1 method in describing the conformational behavior of nylons has been recently proved.[22,37,38] Indeed, this method was designed by Dewar and co-workers with the aim of providing

reliable geometrical and conformational trends.[35] On the other hand, the PM3 method was developed to predict accurately hydrogen bond energies.[22] Energy calculations were carried out using the refined LALS geometries.

Two different kinds of calculations were performed. First, the conformational energy for the different models was computed considering an isolated polymer chain. For this purpose, energy calculations of the compounds H[NHCO(CH₂)₃CONH-(CH₂)₅]ₙH, where n varies from 1 to 5, were performed. For each of these compounds the models were built by repeating forms of the same conformation, i.e., assigning to each residue of the chain the same conformational angles. Second, the energy of the crystal for the different models was evaluated at the same level of theory. The energy of the crystal for one residue in a single chain was estimated by

$$E_{\text{crystal}} = E_0 + {}^1\!/_2 \sum_j E_{ij} \qquad (1)$$

where E_0 is the conformational energy of a residue and E_{ij} is the interaction energy between the residue i and all the nearest neighbor residues j. Due to the large amount of computer resources required by quantum mechanical calculations, even at the semiempirical level, interactions between residues other than nearest neighbor are neglected.

Semiempirical calculations were performed with a locally modified version of the MOPAC program[39] using the standard AM1[35] and PM3[36] parameters. Calculations were performed on a CRAY-YMP at the "Centre de Supercomputació de Catalunya" (CESCA).

Results and Discussion

Synthesis and Characterization. Interfacial polymerization gives nylon 55 in a 40% yield. Elemental anal. Calcd for C₁₀H₁₈N₂O₂: C, 60.61; H, 9.09; N, 14.14. Found: C, 61.42; H, 9.49; N, 13.90. The intrinsic viscosity (0.55 dL/g, measured in dichloroacetic acid at 25 °C) corresponds to a molecular weight of about 9400 (DP 47) if the viscosimetric equation of nylon 66[40] is applied for calculation.

The infrared spectrum of nylon 55 shows characteristic amide and methylene absorption bands: 3295 (amide A), 3091 (amide B), 2931 and 2858 (C−H), 1638 (amide I) and 1542 cm⁻¹ (amide II). Inspection of the region between 800 and 500 cm⁻¹, which is highly sensitive to the crystalline structure of nylons, shows peaks at 628 and 591 cm⁻¹. They may be attributed as a first approximation to the amide VI mode of both γ and α structures which for nylon 6[41] appear at 630 and 580 cm⁻¹, respectively. The chemical shifts of the intense signals observed in the ^{1}H and ^{13}C NMR spectra are in full agreement with the anticipated chemical composition: ^{1}H NMR (300.1 MHz, TFA-*d*) δ 1.54 (2H, m, NHCH₂CH₂C*H*₂), 1.83 (4H, m, NHCH₂C*H*₂), 2.23 (2H, m, COCH₂C*H*₂), 2.84 (4H, t, COCH₂), 3.57 (4H, t, NHC*H*₂); ^{13}C NMR (75.5 MHz, TFA-*d*) δ 23.20 (COC-H₂*C*H₂), 25.59 (NHCH₂CH₂*C*H₂), 29.60 (NHCH₂*C*H₂), 34.29 (CO*C*H₂), 43.66 (NH*C*H₂), 179.75 (*C*ONH). Furthermore, no signs of branching or irregularities are detected in the NMR spectra.

Thermal Behavior. Figure 2 shows the sequence of four DSC scans performed with the sample crystallized directly from the synthesis mixture. In the first run (a) the sample was heated (20 °C/min) through fusion and left in the melt for 2−3 min, and then it was cooled (20 °C/min) to observe crystallization from the melt (run b). A second heating (run c) and a second cooling (run d) were done in order to check the reproducibility of the transitions and get data for the melt-crystallized samples. A double melting endotherm (216 and 237 °C) is seen for the solution-crystallized
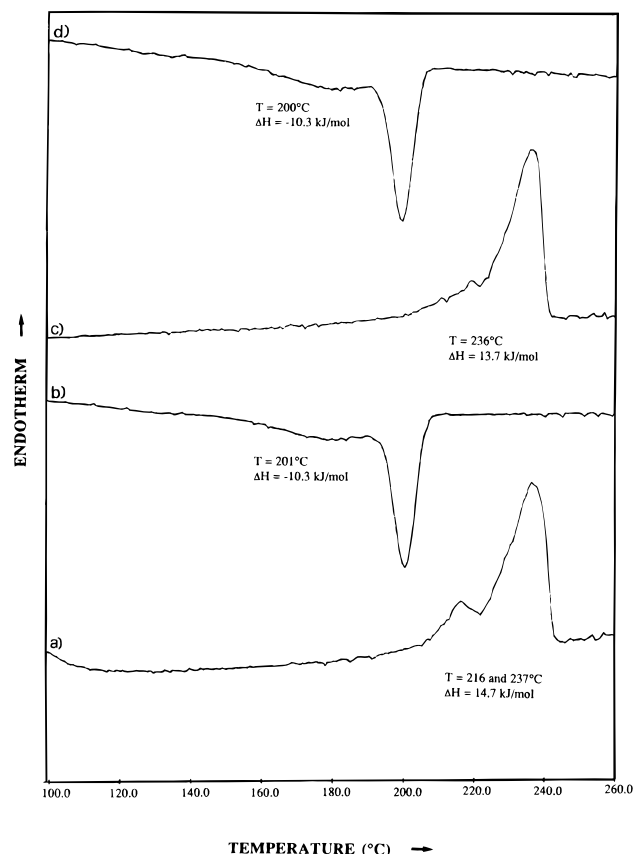
Figure 2. Sequence of four DSC traces for solution-crystallized nylon 55 obtained at a rate of 20 °C/min: run a, heating of the original sample; run b, cooling; run c, reheating; run d, recooling after the second heating.

Figure 3. Transmission electron micrographs of nylon 55 obtained from formic acid−butanol solutions, illustrating the different morphologies observed: (a) rhombic crystals; (b) oval-shaped crystals; (c) lath-shaped lamellae. Scale bar = 1 μm.

sample, a very common observation in thermal studies of nylons. The measured melting temperatures are compatible with the literature data reported for nylon 55 (247 °C).[32] The melting temperatures are lower than expected when compared with those of similar even−even nylons (i.e., 265 °C for nylon 66[1]), suggesting a different structure or differences in chain mobility.

The DSC traces shown in Figure 2 indicate thermal stability, since the transition observed on heating is reproducible. Comparison between traces a and c of Figure 2 indicates a greater reorganization during heating for the melt-crystallized samples or a preferential crystallization from the melt in the high-temperature state. In order to evaluate the crystallinity of nylon 55 we estimate the equilibrium heat of fusion (ΔH_f^{eq}) as a first approximation. A ΔH_f^{eq} of 36.2 kJ/mol was calculated using the reported[42] group contributions of the amide (2.0 kJ/mol) and the methylene (4.0 kJ/mol) groups. Thus crystallinities around 40% and 38% were evaluated for the solution and melt-crystallized samples, respectively.

Morphology. Precipitation of nylon 55 from formic acid−butanol solutions at 110 °C rendered a wide diversity of morphologies. Their relative proportion varies from one preparation to another depending on the proportion of the precipitating agent (butanol).

Rhombus-shaped crystals (Figure 3a) dominate the preparations obtained when 3 volumes of butanol was poured into a 1% solution of nylon 55 in formic acid. These crystals were flat in appearance since no striation, indicative of pyramidal structures which collapse on sedimentation, has been detected. Overgrowth of lamellae ca. 75 Å thick (as estimated from their shadow
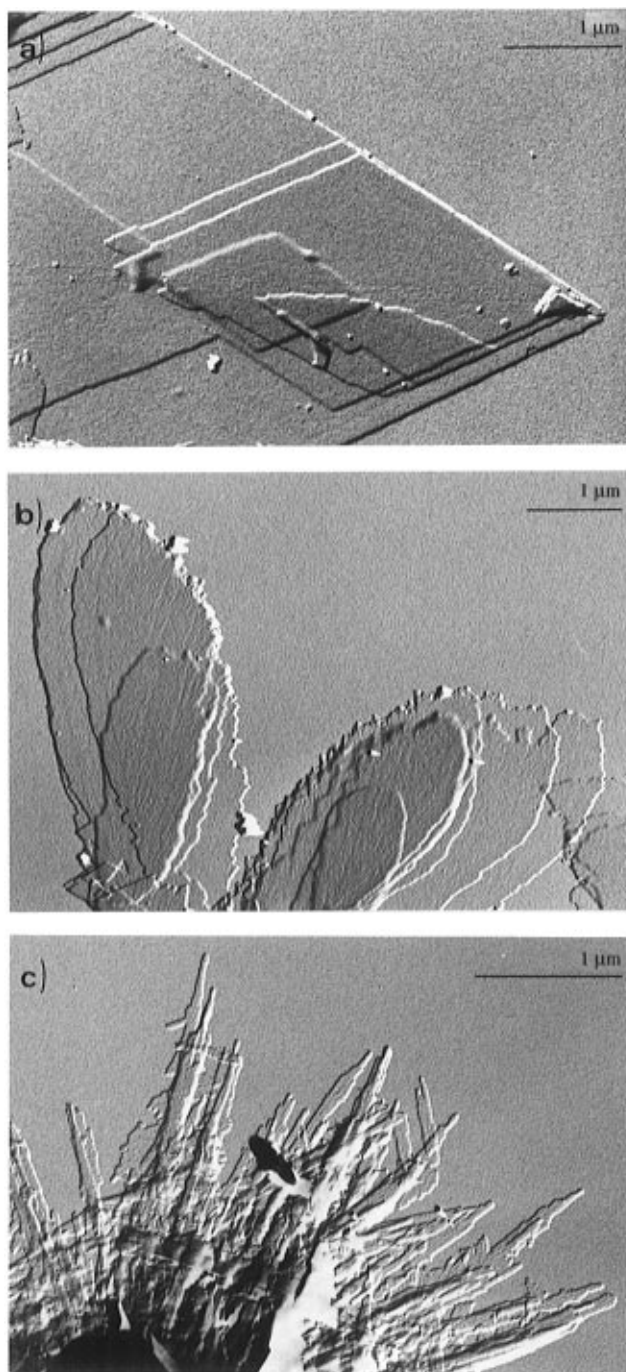
in the micrographs) is usually observed. It is worth noting both the large dimensions of single crystals (more than 10 μm long) and the highly regular edges which form angles of 60° and 120°. On the contrary, crystals with serrated growth faces were preferably developed when more than 4 volumes of butanol was added in the crystallization medium. In this case, precipitation proceeded faster and the resulting crystals were oval in appearance (Figure 3b), although their dimensions were comparable with those of the rhombus-shaped crystals. Spherulitic aggregates composed of lath-shaped lamellae (Figure 3c) were also attained under both sets of crystallization conditions.

It is also interesting to note that the rhombic crystals become more irregular as the butanol content increases.
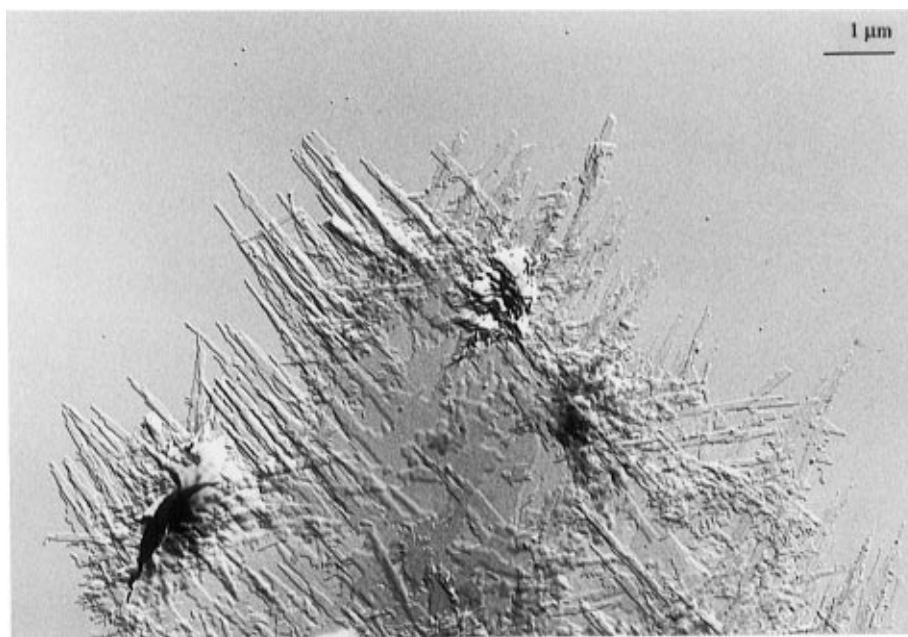
Figure 4. Transmission electron micrograph of an irregular lamella obtained from solutions with high water content. Note that lath-like protuberances develop at each side of the rhombic crystal. Irregular edges are characteristic of individual lamellae. Scale bar = 1 μm.
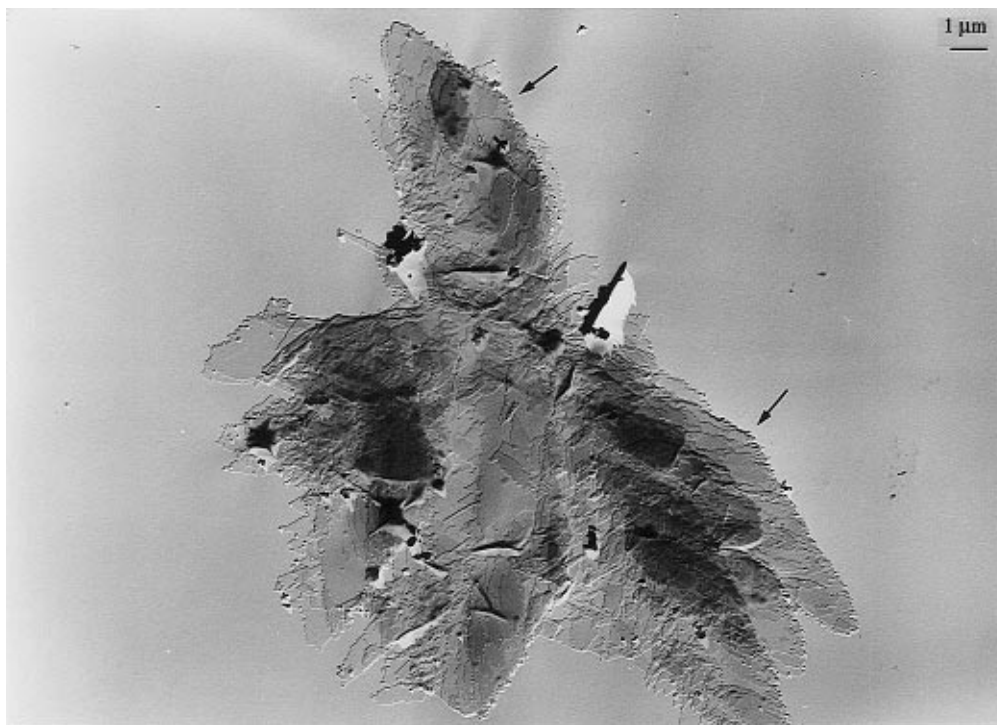
Figure 5. Transmission electron micrograph of a complex aggregate obtained from solutions with high water content. Note the presence of irregular crystals whose morphology is intermediate between rhombic and oval-shaped. Arrows indicate angles close to 120°. Scale bar = 1 μm.

Thus Figure 4 shows a crystalline aggregate, obtained in a formic acid–butanol (1:4, v/v) mixture, where the rhombic geometry is still recognizable. In fact the aggregate is composed of individual lamellae with very irregular edges. These lamellae grow according to one preferred direction which runs in parallel to either side of the rhombic crystal. Therefore, irregular and lath-shaped protuberances (similar to those observed in the spherulitic aggregates) develop on each side of the crystal.

The rhombic and the oval-shaped crystals are also related. The complex aggregate shown in Figure 5 is composed of irregular lamellar crystals whose shape is intermediate between rhombic and oval. Thus angles close to 120° and 60° are still recognizable. Furthermore, some of the basal lamellae consist of growth twins where the rhombic habit is obvious. Note also that some crystals are preferably developed in one direction, giving lath-shaped lamellae.

Electron Diffraction. The diffraction patterns obtained from the various types of single crystals are identical. They are characterized by a pseudohexagonal arrangement of the diffraction spots. They usually extend out to 5 orders of the basic spacing at 4.15 Å, which indicates that the crystal structure is well preserved to near 0.83 Å resolution. The diffraction

Table 1. Measured and Calculated X-ray Diffraction Spacings d_B (Å) for Different Nylon 55 Samples: Powder Recovered from Synthesis, Mat of Sedimented Crystals Obtained from a Formic Acid−Water (1:3) Solution, and Fiber Annealed at 140 °C

index[a]	calcd	powder		crystal mat[b]			annealed fiber[b]		
lamellar thickness	76			78[c]	s				
second-order lamellar thickness	38			38[c]	w				
001	13.8	13.6	m	14.0	m	M	13.5	s	M
subsidiary maxima	10.6, 9.2, 8.1	10.8, 8.9	vw	10.9, 9.3, 8.3	vw	M			
002	6.90	6.90	m	7.00	m	M	6.80	s	M
subsidiary maxima	6.00, 5.53, 5.11			6.11, 5.50, 5.01	vw	M			
003	4.60	4.61	w	4.55	w	M	4.56	w	M
100	4.15	4.15	vs	4.15	vs	E	4.15	vs	E
101	3.97	3.88	s	3.89	s		3.95	m	off M
102, 004	3.56, 3.45	3.52	w	3.43	m				
103	3.08	3.05	vw	3.04	w				
005	2.76			2.80	w				
104	2.65	2.66	vw	2.58	w				
110, 111	2.40, 2.36	2.41	m	2.41	m				
105, 112	2.30, 2.27	2.26	vw	2.26	w				
113	2.13			2.12	w				

[a] On the basis of a primitive monoclinic cell: $a = b = 4.79$ Å, $c = 13.8$ Å; $\alpha = \beta = 90°$, $\gamma = 120°$. [b] Abbreviations denote intensities or orientation: vs, very strong; s, strong; m, medium; w, weak; vw, very weak, M, meridional; E, equatorial; off M, off meridonal. [c] Observed only in low-angle X-ray patterns.
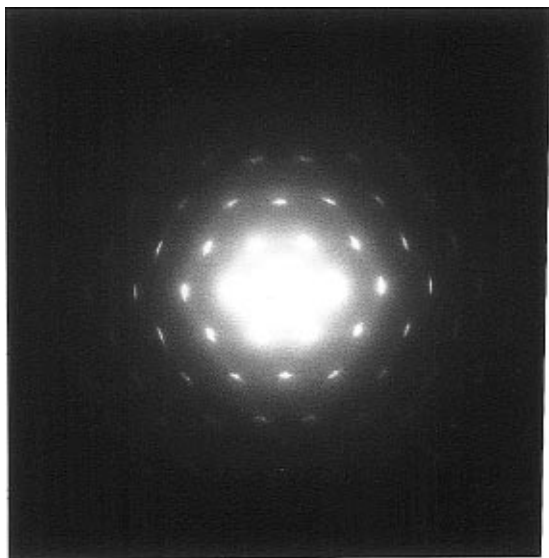
Figure 6. Selected area diffraction patterns from crystals of nylon 55. The two most intense reflections appear oriented in the direction of the long axis of the rhombic crystals.

pattern of the rhombic crystals is characterized by the fact that two of the six inner spots are the most intense (Figure 6) and appear oriented in the direction of the long axis of the crystals. A hexagonal symmetry has never been detected in the different patterns obtained, allowing us to disregard models with either a regular or a random arrangement of three hydrogen bond directions. In all cases the patterns exhibit an *mm* symmetry (or very close to it). This lack of hexagonal symmetry is in agreement with the nonhexagonal morphology exhibited by the crystals.

From the *hk*0 lattice spacings, the values of the projected cell can be calculated. Thus we can deduce either a primitive ($a = 4.79$ Å, $b = 4.79$ Å, and $\gamma = 120°$) or a centered cell ($a = 8.30$ Å, $b = 4.79$ Å, and $\gamma = 90°$) which appears more consistent with symmetry considerations as will be discussed in later sections. Furthermore, it is evident from the *hk*0 diffraction pattern that the molecular chains are folded as a consequence of the reduced lamellar thickness.

X-ray Diffraction Data. A unique structure may be inferred from the analysis of the diffraction patterns

(Figure 7) of different nylon 55 samples: (a) powder recovered directly from the synthesis medium, (b) mat of sedimented single crystals obtained from a formic acid−butanol (1:3, v/v) solution, and (c) fibers prepared from the melt and annealed at 140 °C under stress. The measured spacings are similar within experimental error and can be indexed with either a primitive unit cell ($a = b = 4.79$ Å; $c = 13.8$ Å; $\alpha = \beta = 90°$ and $\gamma = 120°$; Table 1) or a centered one ($a = 8.30$ Å; $b = 4.79$ Å; $c = 13.8$ Å; $\alpha = \beta = \gamma = 90°$). The unit cells agree with the values deduced from the electron diffraction patterns and suggest a structure related to the γ-form. In fact a shortening in the molecular unit length with respect to an extended conformation may be deduced from the c parameter. This decrease, about 0.5 Å/amide group, is close to the characteristic value for a γ-structure. The density calculated for the proposed unit cell dimensions is 1.18 g/cm³, while the measured density is about 1.06 g/cm³. Thus a satisfactory agreement is found if we take into account the expected decrease in density due to the presence of ca. 60% amorphous material (estimated from calorimetric data). The nylon 55 structure seems to be stable over the whole temperature range between room temperature and the melting temperature, since no change of the measured *d*-spacings was detected in the fiber diffraction patterns registered at different temperatures. Some additional features derived from the diffraction patterns are the following:

(a) Mats from single crystals, obtained from a formic acid−butanol (1:3, v/v) solution, exhibited a moderate orientation. However, broad meridional reflections at 78 and 38 Å were detected in the low-angle patterns. These reflections arise from the stacking of lamellae, and they are assigned to the first and second lamellar orders. The derived lamellar thickness is similar to the value measured by electron microscopy and corresponds to about 5.6 repeat units.

(b) Weak and sharp reflections were observed between the 00*l* spacings in the patterns obtained from powders or sedimented crystals. Thus three reflections with an approximate meridional orientation have been measured between the 001 and 002 spacings (and also between the 002 and 003 spacings). This pattern of subsidiary maxima is commensurate with five monomer
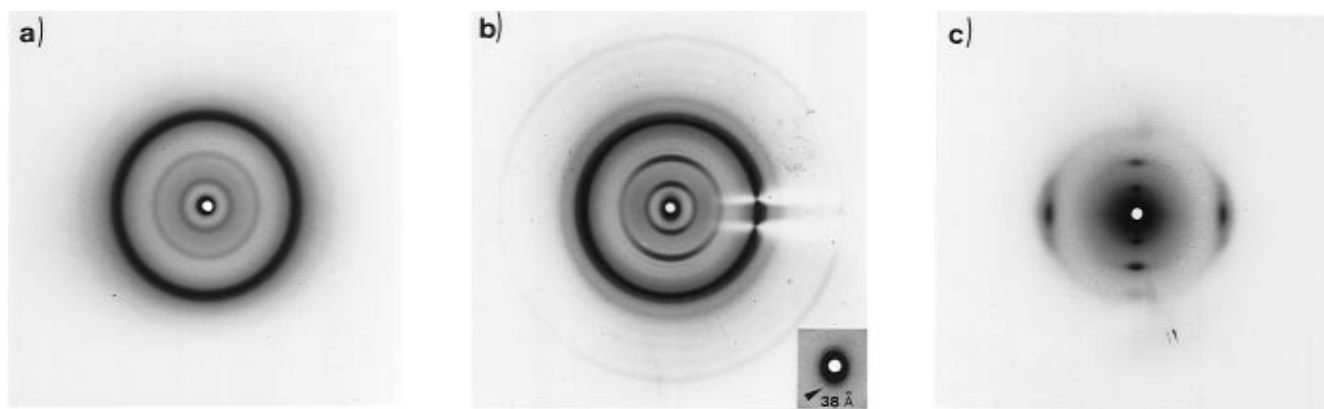
Figure 7. X-ray diffraction patterns of nylon 55: (a) powder recovered from synthesis; (b) mat of sedimented crystals obtained from formic acid−water (1:3, v/v) solution; a meridional reflection (38 Å) related to the lamellar thickness is present in the low-angle pattern (inset); (c) fiber obtained from the melt and annealed at 140 °C (draw ratio 2.5×).

Table 2. Conformational Parameters and Hydrogen Bond Geometry for Models of Nylon 55

	model I	model II
molecular symmetry	m	2
space group	$P11m$	$C121$
torsional angles (deg)		
φ_1	108.8	−107.6
φ_2	−108.8	−107.6
ψ_1	120.0	101.8
ψ_2	−120.0	101.8
ν_i	180.0	180.0
ω_i	180.0	180.0
hydrogen bond geometry		
d(H···O) (Å)	1.80	1.94
d(N···O) (Å)	2.67	2.90
∠NHO (deg)	142.5	158.0
R factor		
X-ray diffraction data (%)	22	20
electron diffraction data (%)	38	15
crystal energy (kcal/mol)		
AM1 method	−0.4	−11.6
PM3 method	−8.9	−14.2

repeating units, in a similar way to that suggested for nylon 66 by Atkins *et al.*[43] The visibility of these maxima in itself implies a significant uniformity of the crystal core.

(c) The most intense reflection corresponds to the 100 chain packing spacing (indexed using the primitive unit cell) and has an equatorial orientation in both fiber and sedimented crystal patterns.

(d) The fiber pattern has features similar to those of the conventional γ-form of nylons, although the number of reflections observed is limited. Thus the 00*l* reflections appear on the meridian, and a monoclinic unit cell with α = β = 90° may be inferred. This situation contrasts with the related polymer nylon 65,[30] where molecular chains are shifted in order to optimize the hydrogen bond geometry.

(e) All reflections can be indexed with a c parameter equivalent to only one chemical repeat distance. Only the indexing of the 2.80 Å reflection (005 spacing) is doubtful, since no orientation can be established. Note that a double value for the c parameter is necessary to index the reflection as a 10*l* spacing.

Structural Modeling. Although the fiber diffraction pattern of nylon 55 suggests a conventional γ-form, there are some considerations that make this structure unlikely:

(a) A $P11m$ space group is expected for a γ-form of nylon 55 (as established by Kinoshita[31] for the similar polymer nylon 77). Thus the $hk0$ electron diffraction pattern should have a 2 symmetry in contrast with the experimental observations. An *mm* symmetry becomes only possible for a γ-form when we consider unit cells with more than one molecular chain in the unit cell. However, the different models tested on this basis are characterized by X-ray and electron diffraction patterns with reflections additional to those observed.

(b) Lamellar crystals have an unusual stability to the electron beam since up to 5 diffraction orders have been detected in the corresponding diffraction patterns. On the contrary poor diagrams are normally obtained with nylons in which the γ-form is well established.[44,45] In this sense we believe that a structure with two hydrogen bond directions will afford an increased stability.

(c) Recent studies on polyamides[22,30] and model oligoamides[28] derived from glutaric acid suggest that their two C−O directions tend to be rotated, giving structures with two hydrogen bond directions. In fact a parallel orientation of the carbonyl groups, as expected for a γ-form, is energetically unfavored.

Taking into account these considerations we have modeled a new structure for nylon 55 (model II), which was then compared with a conventional γ-form (model I). Molecular drawings of lateral and equatorial projections of both structures are shown in Figure 8, whereas in Table 2 the two structures are compared.

The molecular symmetry of model I is characterized by mirror planes perpendicular to the chain axis through every central carbon atom between the amide groups, and it is attained when $\varphi_1 = -\varphi_2$ and $\psi_1 = -\psi_2$. The refined torsional angles (±108° to ±120°) are similar to those reported for other nylons in the γ-form and produce a tilting of the amide plane with respect to the chain axis which allows the formation of hydrogen bonds with an NH···O distance of approximately 1.8 Å and which is close to linear. All the carbonyl groups in the primitive unit cell point in the same direction, and so the structure should be electrically active.

The molecular symmetry of model II is characterized by two parallel binary axes perpendicular to the chain direction through the central carbon atom of both diamine and diacid moieties. This symmetry maintains the adirectional configuration of the polymer, and it is attained when $\varphi_1 = \varphi_2$ and $\psi_1 = \psi_2$. Moreover, the rotation between the amide groups induced by the carbonyl moiety can be compensated by a rotation in the opposite sense induced by the diamine moiety, when φ_i and ψ_i have opposite signs. Note also that the absolute values of all refined torsional angles are close to those expected for a γ-structure. The main difference between models I and II is the fact that the torsional

a)

b)

c)

d)
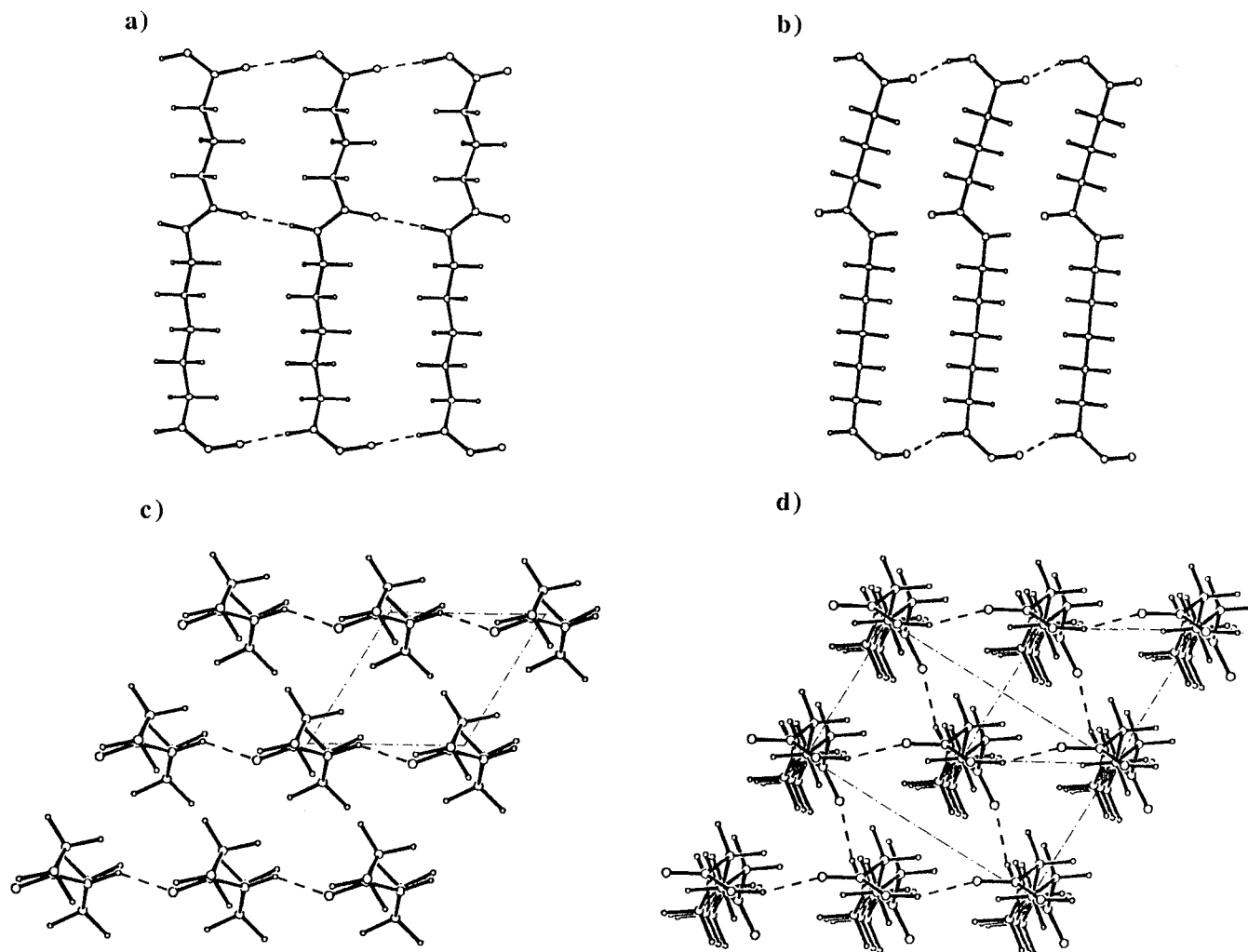
Figure 8. Side view of three molecular chains which are hydrogen bonded along the *a* direction: (a) model I; (b) model II. Equatorial projections of nine neighboring chains: (c) model I; (d) model II. Hydrogen bonds, indicated by dashed lines, are established in a single direction in model I, whereas two hydrogen bond directions are characteristic of model II. Unit cell contours are indicated in parts c and d with thinner lines. Both primitive and centered unit cells are indicated in part d.

angles φ_i and ψ_i of alternate amide groups have opposite signs. The model II also appears stereochemically suitable and shows no significant contacts. Hydrogen bonds with length and angle values within the standard range are formed in two directions approximately rotated 120°. A net dipolar moment is expected for the unit cell, so that the polymer should also be electrically active. Note also that a centered unit cell and a $C121$ space group are expected for model II according to its molecular symmetry.

The observed and calculated structure factors of the reflections used in the X-ray and electron diffraction analyses are given in Tables 3 and 4. In some cases several hkl planes contribute to the calculated structure factors due to the pseudohexagonal cell. The values of F_c listed in Table 3 include the contributions of such planes. Both models give acceptable and similar disagreement R factors ($\Sigma|F_o - F_c|/\Sigma F_o$) for X-ray analysis (about 20%); however, the calculated R factor for electron diffraction clearly points to model II (15% versus 38%), as expected from symmetry considerations. The orientation of the lattice with respect to the crystal, as deduced from the relative orientation of the electron diffraction pattern, is such that the two hydrogen bond directions of model II run parallel to the crystal edges. Thus the protuberances observed in the irregular crystals depicted in Figure 4 can be well explained, assum-

**Table 3. Observed (F_o) and Calculated (F_c) X-ray Structure Factors for Models of Nylon 55**

ring	d(calcd) (Å)	hkl[a]	m[b]	F_o	model I	model II
					F_c[c]	
1	13.8	001	1	10	5.3	7
2	6.90	002	1	17	15	12
3	4.60	003	1	13	12.5	13
4	4.15	100, 010, $\bar{1}$10	1,1,1	75	68	73
5	3.97	101, 011, $\bar{1}$11	2,2,2	43	50	35
6	3.56	102, 012, $\bar{1}$12	2,2,2	32	26	43
	3.45	004	1			
7	3.08	103, 013, $\bar{1}$13	2,2,2	20	31	27
8	2.76	005	1	10	13	10
9	2.65	104, 014, $\bar{1}$14	2,2,2	15	17	29
10	2.40	110, $\bar{1}$20, $\bar{2}$10	1,1,1	40	32	34
	2.36	111, $\bar{1}$21, $\bar{2}$11	2,2,2			
11	2.30	105, 015, $\bar{1}$15	2,2,2	35	44	40
	2.27	112, $\bar{1}$21, $\bar{2}$11	2,2,2			
12	2.13	113, $\bar{1}$23, $\bar{2}$13	2,2,2	30	15	22

[a] For comparative purposes we use for both models the same primitive unit cell ($a = b = 4.79$ Å, $c = 13.8$ Å; $\alpha = \beta = 90°$, $\gamma = 120°$). [b] Multiplicity. [c] Calculated as $F_c = (\Sigma m_{hkl} F_{chkl}^2)^{1/2}$.

ing that hydrogen bonds correspond to the preferential growing direction.

Simulated diffraction patterns of both models are shown in Figure 9. Powder and fiber X-ray patterns are very similar, while larger differences can be ap-
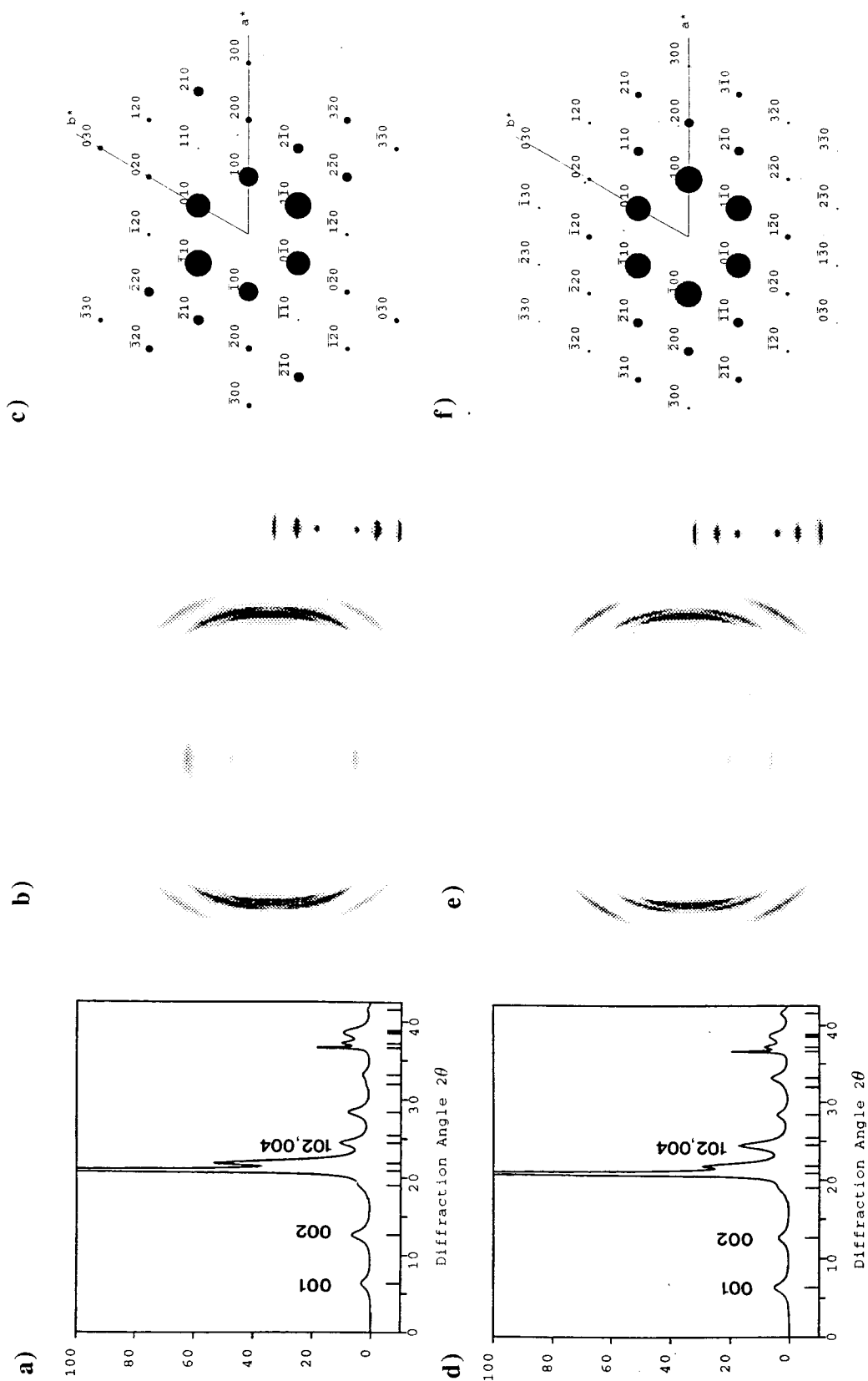
Figure 9. Simulated diffraction patterns for the two models of nylon 55: (a–c) model I; (d–e) and model II. Only the most distinctive reflections are labeled in the X-ray powder diffraction profiles a and d. The inset of the X-ray fiber diffraction patterns b and e corresponds to the meridional reflections. Note the different symmetry of the hk0 electron diffraction pattern of single crystals shown in c and f. For comparative purposes the reflections of both models have been indexed on the basis of the same primitive unit cell.

Table 4. Observed (F_o) and Calculated (F_c) Electron Diffraction Structure Factors for Models of Nylon 55

spot	d(calcd) (Å)	hkl[a]	F_o	F_c model I	F_c model II
1	4.15	100	23.0	15.1	21.6
2	4.15	010	18.0	19.8	20.0
3	4.15	$\bar{1}$10	18.0	22.0	20.0
4	2.40	110	8.0	1.7	6.8
5	2.40	$\bar{1}$20	4.0	2.4	3.7
6	2.40	$\bar{2}$10	8.0	6.0	6.8
7	2.07	200	9.0	5.3	6.0
8	2.07	020	3.0	3.5	2.7
9	2.07	$\bar{2}$20	3.0	8.2	2.7
10	1.57	210	4.0	5.6	3.3
11	1.57	120	2.0	1.5	2.3
12	1.57	$\bar{1}$30	2.0	0.7	1.5
13	1.57	$\bar{2}$30	2.0	1.6	1.5
14	1.57	$\bar{3}$20	2.0	2.2	2.3
15	1.57	$\bar{3}$10	4.0	1.3	3.3
16	1.38	300	2.0	2.9	1.0
17	1.38	030	1.0	2.2	0.9
18	1.38	$\bar{3}$30	1.0	2.3	0.9

[a] For comparative purposes we use for both models the same primitive unit cell ($a = b = 4.79$ Å, $c = 13.8$ Å; $\alpha = \beta = 90°$, $\gamma = 120°$).
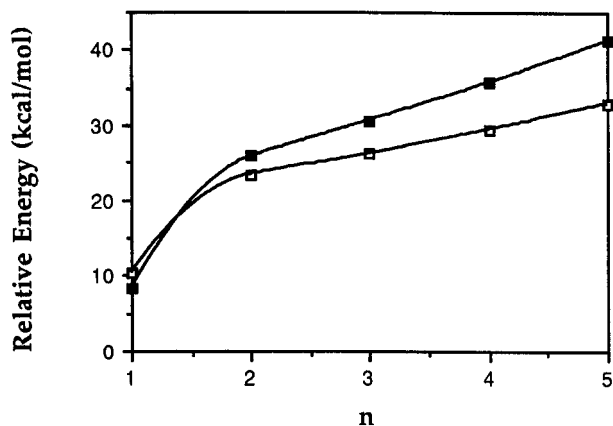
Figure 10. Energy difference between models I and II as function of the number of residues of the molecular chain (n) calculated with the (■) AM1 and (□) PM3 methods as described in the text.

preciated in the electron diffraction patterns. However, it is interesting to note that the main differences in the powder diffraction profiles consist in the relative intensities of the 001 and 002 reflections and also the appreciable intensity of the 3.6−3.4 Å reflection (102 and 004 planes). With these observations taken into account, model II is favored, since diffraction patterns show the predominance of the 001 reflection over the 002 reflection (Figure 7a) and also of the 3.6−3.4 Å reflection over its neighbors (Figure 7b).

Energy Calculations. The conformational energies of the two proposed models were computed for H[NHCO-(CH$_2$)$_3$CONH(CH$_2$)$_5$]$_n$H, where n ranges from 1 to 5, using AM1 and PM3 calculations. Figure 10 shows the variation of the relative conformational energy between models I and II with chain length for the two computational methods. For all the values of n considered, model I is less favored from a conformational point of view; model II appears to be the more stable one.

The present calculations permit the investigation of cooperative energy effects in models I and II that would reverse the energy order between both conformations when the value of n increases. Thus, the difference between the energy of compounds with $n = 2$ and $n = 3$ in a defined conformation can be associated with a residue energy increment (REI) that results when a single residue fragment is inserted into a polymer chain with the same conformation.[46−48] The REI values computed with the AM1/PM3 methods are −88.6/−89.7 kcal/mol for model I; and −93.4/−91.5 Kcal/mol for model II. These values indicate that the insertion of a residue fragment into a polymer chain with the conformation of model I is 4.8/1.8 kcal/mol less favored than with the conformation of model II. If the total energy, for a characteristic conformation, does not contain any cooperative effects, then the energy can be predicted with the following equation:[46−48]

$$E^{\text{predicted}}(n = N) = (N - 2)(\text{REI}) + E(n = 2)$$

In particular for the compound with $n = 5$, the predicted AM1/PM3 energies are −442.7/−441.5 kcal/mol and −483.1/−470.3 kcal/mol for models I and II, respectively, whereas the quantum mechanical calculated values are −442.2/−438.1 kcal/mol and −483.4/−471.1 kcal/mol. The difference between the predicted and the quantum mechanical computed energies gives the cooperative energy difference.[46−48] Thus, no cooperative energy effect is detected at the PM3 level for the conformation of model I (+3.4 kcal/mol). Consequently, the present calculations clearly indicate that no change in the respective conformational energy of models I and II is expected when the number of residues in the polymer chain increases.

The energy of the crystal for models I and II estimated by eq 1 is included in Table 2. It is worth noting that model II is again favored over model I, the relative energies being 11.2 kcal/mol and 5.3 kcal/mol at the AM1 and PM3 levels, respectively. Differences between AM1 and PM3 must be basically attributed to the different treatment of the interactions. Thus, the interchain energy is given by the interactions with the hydrogen-bonded chains and by the van der Waals contacts with the remainder of adjacent chains. AM1 and PM3 interaction energies with the hydrogen-bonded chains are quite similar, whereas the two methods provide different van der Waals interaction energies. The AM1 method gives positive energies which indicate hard repulsive interactions, whereas the PM3 Hamiltonian gives a zero or soft interaction.

Conclusions

The results of the present study can be summarized as follows:

(1) From X-ray and electron diffraction patterns we have determined that the crystal structure of nylon 55 can be represented by either a primitive unit cell with parameters $a = b = 4.79$ Å, $c = 13.8$ Å, $\alpha = \beta = 90°$, and $\gamma = 120°$ or a centered unit cell with parameters $a = 8.30$ Å, $b = 4.79$ Å, $c = 13.8$ Å, and $\alpha = \beta = \gamma = 90°$.

(2) The morphology of the lamellar crystals greatly depends on the crystallization conditions. However, a lamellar thickness close to 76 Å is characteristic for the different crystals obtained from formic acid−butanol solutions.

(3) Subsidiary maxima indicate that the crystals have a regular core constituted by five repeating units.

(4) A new model based on two hydrogen bond directions fits better with the experimental data than a conventional γ-form. The glutaryl units take a particular conformation where the two carbonyl directions are rotated. A similar but opposite rotation is also charac-

teristic of the diamine moiety. The resulting space group is *C*121.

(5) Energy calculations on isolated molecular chains clearly indicate that the conformation based on a γ-form is unfavored with respect to this new structure based on two hydrogen bond directions. Similar results are derived from packing analysis where van der Waals interactions seem to have a significant influence.

References and Notes

(1) Miller, R. L. *Polymer Handbook*, 3rd ed.; Brandrup, J., Immergut, E. H., Eds.; Wiley Interscience: New York, 1989; Chapter VI.
(2) Arimoto, H. *J. Polym. Sci., Part A: Gen. Pap.* **1964**, *2*, 2283.
(3) Ziabicki, A.; Kedzierska, A. *J. Appl. Polym. Sci.* **1959**, *2*, 14.
(4) Stepaniak, R. F.; Garton, A.; Carlsson, D. J.; Wiles, D. M. *J. Polym. Sci., Polym. Phys.* **1979**, *17*, 987.
(5) Illers, H. K.; Haberkorn, H.; Simak, P. *Makromol. Chem.* **1972**, *158*, 285.
(6) Hiramatsu, N.; Harguchi, K.; Hirakawa, S. *Jpn. J. Appl. Phys.* **1983**, *22*, 335.
(7) Attkins, E. D. T.; Hill, M. J.; Veluraja, K. *Polymer* **1995**, *36*, 35.
(8) Brill, R. *J. Prakt. Chem.* **1942**, *161*, 49.
(9) Radusch, H. J.; Stolp, M.; Androsch, R. *Polymer* **1994**, *35*, 3568.
(10) Brill, R. *Makromol. Chem.* **1956**, *18*, 294.
(11) Hirschinger, J.; Miura, H.; Gardner, K. H.; English, A. D. *Macromolecules* **1990**, *23*, 2153.
(12) Colclough, M. L.; Baker, R. *J. Mater. Sci.* **1978**, *13*, 2531.
(13) Puiggalí, J.; Muñoz-Guerra, S.; Lotz, B. *Macromolecules* **1986**, *19*, 1119.
(14) Puiggalí, J.; Muñoz-Guerra, S.; Subirana, J. A. *Polymer* **1987**, *28*, 209.
(15) Bella, J.; Puiggalí, J.; Subirana, J. A. *Polymer* **1994**, *35*, 1231.
(16) Bermúdez, M.; Puiggalí, J.; Muñoz-Guerra, S. *Macromolecules* **1994**, *27*, 6325.
(17) Puiggalí, J.; Subirana, J. A. *Polymeric Materials Encyclopedia*; Salomone, J. C., Ed.; CRC Press: Boca Raton, in press.
(18) Aceituno, J. E.; Subirana, J. A. Electron Mycroscopy. In *EUREM 92*; López-Galindo, A., Rodriguez-García, M. I., Eds.; Publicaciones de la Universidad de Granada: Granada, 1992; Vol. 2, p 375.
(19) Aceituno, J. E.; Tereshko, V.; Lotz, B.; Subirana, J. A. In preparation.
(20) Franco, L.; Aceituno, J. E.; Subirana, J. A.; Puiggalí, J. *Polym. Prepr.* **1992**, *31*, 325.
(21) Franco, L.; Navarro, E.; Subirana, J. A.; Puiggalí, J. *Macromolecules* **1994**, *27*, 4284.
(22) Alemán, C.; Franco, L.; Puiggalí, J. *Macromolecules* **1994**, *27*, 4298.
(23) Tormo, J.; Puiggalí, J.; Vives, J.; Fita, I.; Lloveras, J.; Bella, J.; Aymamí, J.; Subirana, J. A. *Biopolymers* **1992**, *32*, 643.
(24) Tereshko, V.; Navarro, E.; Puiggalí, J.; Subirana, J. A. *Macromolecules* **1993**, *26*, 7024.
(25) Navarro, E.; Puiggalí, J.; Subirana, J. A. *Makromol. Chem. Phys.* **1995**, *196*, 2361.
(26) Navarro, E.; Tereshko, V.; Subirana, J. A.; Puiggalí, J. *Biopolymers* **1995**, *36*, 711.
(27) Tereshko, V.; Vidal, X.; Goodman, M.; Subirana, J. A. *Macromolecules* **1995**, *28*, 264.
(28) Navarro, E.; Alemán, C. Puiggalí, J. *J. Am. Chem. Soc.* **1995**, *117*, 7307.
(29) Alemán, C.; Navarro, E.; Puiggalí, J. *J. Org. Chem.* **1995**, *60*, 6135.
(30) Navarro, E.; Franco, L.; Subirana, J. A.; Puiggalí, J. *Macromolecules* **1995**, *28*, 8742.
(31) Kinoshita, Y. *Makromol. Chem.* **1959**, *33*, 1.
(32) Magill, J. H. *J. Polym. Sci., Part A-2* **1971**, *9*, 815.
(33) Dreyfuss, P. *J. Polym. Sci., Polym. Phys. Ed.* **1973**, *11*, 201.
(34) Campbell-Smith, P.; Arnott, S. *Acta Crystallogr., Sect. A* **1978**, *34*, 3.
(35) Dewar, M. J. S.; Zoebisch, E. G.; Healy, E. F.; Steward, J. J. P. *J. Am. Chem. Soc.* **1985**, *107*, 3902.
(36) Steward, J. J. P. *J. Comput. Chem.* **1989**, *10*, 209.
(37) Alemán, C.; Bella, J. *Biopolymers* **1995**, *35*, 257.
(38) Alemán, C.; Puiggalí, J. *J. Org. Chem.* **1995**, *60*, 910.
(39) (a) Steward, J. J. P. *QCPE Bull.* **1983**, *3*, 101. (b) Olivella, S. *QCPE Bull.* **1984**, *4*, 109.
(40) Elias, H. G.; Schumacher, R. *Makromol. Chem.* **1964**, *76*, 23.
(41) Abu-Isa, I. *J. Polym. Sci., Polym. Chem. Ed.* **1971**, *9*, 199.
(42) Van Krevelen, D. W. *Properties of Polymers,* 3rd ed.; Elsevier: Amsterdam, 1990.
(43) Atkins, E. D. T.; Keller, A.; Sadler, D. M. *J. Polym. Sci., Part A-2* **1972**, *10*, 863.
(44) Kyotani, M. *J. Polym. Sci., Polym. Phys. Ed.* **1982**, *20*, 345.
(45) Kawaguchi, A.; Ikawa, T.; Fujiwara, Y.; Tabuchi, M.; Monobe, K. *J. Macromol. Sci. Phys.* **1981**, *B20* (1), 1.
(46) Alemán, C.; Casanovas, J. *J. Comp.-Aided Mol. Des.* **1994**, *8*, 441.
(47) Alemán, C. *Biopolymers* **1994**, *34*, 841.
(48) Alemán, C. *Int. J. Pept. Protein Res.,* in press.

MA960005+